

Tunable Band Gap and Anisotropic Optical Response in Few-layer Black Phosphorus

Vy Tran,¹ Ryan Soklaski,¹ Yufeng Liang,¹ and Li Yang¹

¹*Department of Physics, Washington University in St. Louis, St. Louis, MO 63136, USA*

(Dated: April 18, 2014)

Abstract

We report the quasiparticle band gap, excitons, and highly anisotropic optical responses of few-layer black phosphorous (phosphorene). It is shown that these new materials exhibit unique many-electron effects; the electronic structures are dispersive essentially along one dimension, leading to particularly enhanced self-energy corrections and excitonic effects. Additionally, within a wide energy range, including infrared light and part of visible light, few-layer black phosphorous absorbs light polarized along the structure's armchair direction and is transparent to light polarized along the zigzag direction, making them viable linear polarizers for applications. Finally, the number of phosphorene layers included in the stack controls the material's band gap, optical absorption spectrum, and anisotropic polarization energy-window across a wide range.

PACS numbers:

It is difficult to overstate the interest in graphene and graphene-inspired two-dimensional (2D) crystals [1–3]. Recently, an attractive finite-gapped 2D semiconductor, few-layer black phosphorus (phosphorene), has been successfully fabricated [4–7]. Despite phosphorene’s promising direct band gap, one cannot realistically envision phosphorene devices until its fundamental excited-state properties, such as its quasiparticle (QP) band gap and optical spectrum, are obtained. No such experimental measurements have been made, thus corresponding first-principles predictions are indispensable. Furthermore, these excited-state quantities are known to be dictated by many-electron effects, *e.g.*, electron-electron ($e-e$) and electron-hole ($e-h$) interactions. Therefore, it is essential to turn to *ab-initio* calculations that incorporate many-body self-energy corrections and excitonic effects to advance the forefront of phosphorene research and its applications.

In addition to its direct band gap, few-layer black phosphorus exhibits unique excitonic effects that have not been observed in other 2D structures. For example, recent experiments have observed a strongly anisotropic conducting behavior [5]. It is of particular interest to investigate the effect that this anisotropy has on exciton formation and thus on the excited-state properties of the material. Van der Waals (vdW) interactions allow layers of phosphorene to be stacked; the band gap of the resulting material depends on the number of stacked layers (N) [5, 8]. This has been observed in other 2D semiconductors [9–11]. Because the band gap is a crucial factor in determining electronic screening and corresponding many-electron interactions in the material, the optical spectra and excitonic effects of few-layer phosphorene can also be controlled by the number of stacking layers. Accordingly, studying few-layer phosphorene provides a chance to observe how the electronic structure and excitonic properties of a 2D material transition to that of a 3D material.

In this Letter, we perform first-principles GW-Bethe-Salpeter Equation (BSE) simulations to study the QP band gap and optical spectra of few-layer and bulk black phosphorus, resulting in several important findings. First, we observe significant many-electron effects. For monolayer phosphorene, the self-energy correction enlarges the band gap from 0.8 eV to 2 eV and the lowest-energy optical absorption peak is reduced to 1.2 eV because of a huge exciton binding energy (around 800 meV). These strong many-electron effects result from unique quasi-one dimensional (1D) band dispersions of phosphorene. Second, we observe highly anisotropic optical responses. Few-layer black phosphorus strongly absorbs light polarized along its lattice’s armchair direction, but it is transparent to light polarized along

the zigzag direction. It is chiefly absorbant across the infrared-light range and part of the visible-light range, making it an ideal candidate for being used as an optical linear polarizer with a wide energy window. Finally, the band gap, exciton binding energies, optical absorption spectrum, and linear polarization energy window of phosphorene can all be broadly tuned by changing the number of stacked layers. This serves as a convenient and efficient method for engineering the material’s excited-state properties.

The atomistic ball-stick models of few-layer black phosphorus are presented in Fig. 1 (a) [12, 13]. They are fully relaxed according to the force and stress calculated by density functional theory (DFT) within the PBE functional [14]. The ground-state wave functions and eigenvalues are calculated by DFT/PBE with a k-point grid of 14x10x1 for few-layer structures and 14x10x4 for bulk structures. All calculations use a plane-wave basis with a 25 Ry energy cutoff with a norm-conserving pseudopotential [15]. The QP energy is calculated by the single-shot G_0W_0 approximation with the general plasmon pole model [16]. The involved unoccupied band number is about 10 times of that of valence bands to achieve the converged dielectric function. The excitonic effects are included by solving the BSE with a finer k-point grid of 56x40x1 (35x25x10 for bulk structures) [17]. A slab Coulomb truncation is crucial to mimic suspended structures [18, 19]. Because of the depolarization effect [20, 21], only the incident light polarized parallel with the plane structure is considered in studying optical spectra.

The DFT and QP band structures of monolayer phosphorene are presented in Fig. 1 (b). The band gap is located at the Γ point and the self-energy correction enlarges the band gap from the DFT value of 0.8 eV to 2.0 eV, which is ideal for broad electronic applications [22, 23]. The calculated 150% enhancement is substantially larger than in other 2D semiconductors [24–27]. This is due to the highly anisotropic band structure of the lowest conduction band and highest valence band, as shown in Fig. 1 (b). In particular, the band dispersion is very flat along the $\Gamma - Y$ (zigzag) direction, confining particles to an effective 1D environment along the armchair direction. This effective lower dimension contributes to a larger self-energy correction. The Coulomb truncation is crucial in our calculations of suspended samples. Otherwise, the QP band gap will be substantially smaller, *e.g.*, the monolayer QP band gap will be 1.7 eV. The worse case is that this value fluctuates by different vacuum spacings in simulations.

For multilayer phosphorene, the QP band gap and self-energy corrections vary dramati-

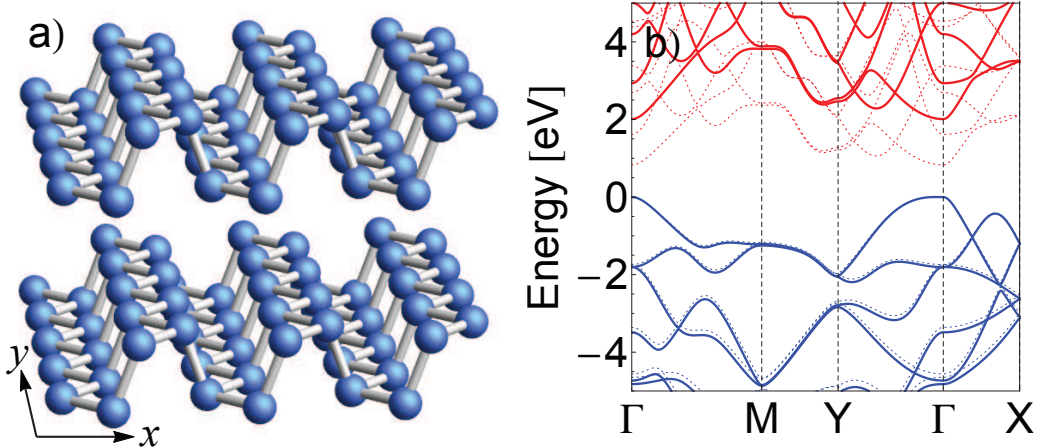


FIG. 1: (Color online) (a) The ball-stick model of few-layer phosphorous. The x axis is perpendicular to and the y direction parallel with the ridge direction, as indicated. (b) The DFT-calculated (dash lines) and GW-calculated (solid lines) band structures of monolayer phosphorous. The top of valence band is set to be zero.

cally according to the stacking layer number, although their band-structure topologies are roughly similar to that of monolayer. As shown in Fig. 2, the QP band gap changes from 2 eV (monolayer) to 0.3 eV (bulk). These bounds provide a wide range of tunability for the band gap and corresponding electronic properties. As an evidence of the reliability of our simulation, our calculated QP band gap of bulk phosphorous is around 300 meV, which is in excellent agreement with experimental results (0.33 eV) [28, 29].

A power law fit of the form $(A/N^\alpha + B)$, where N is the number of layers, is applied in Fig. 2, the results of which are reported in Table I. Surprisingly, the GW-calculated band gaps follows the $1/N^{0.7}$ power law, which decays significantly slower than the usual quantum confinement result ($1/N^2$). This weaker quantum confinement effect results from the vdW interfaces, which partially isolate electrons between neighboring sheets. Another contributing factor may be from the change of the dielectric environment, which is not included in the $1/N^2$ law. It is apparent in Table I and Fig. 2 that the optical absorption peaks and exciton binding energies are affected by the same mechanisms; they follow similar scaling laws with the stacking layer number.

The optical absorption spectra of monolayer, bilayer, trilayer and bulk phosphorene structures are presented in Fig. 3 for incident light polarized along the armchair ($\Gamma-X$) direction.

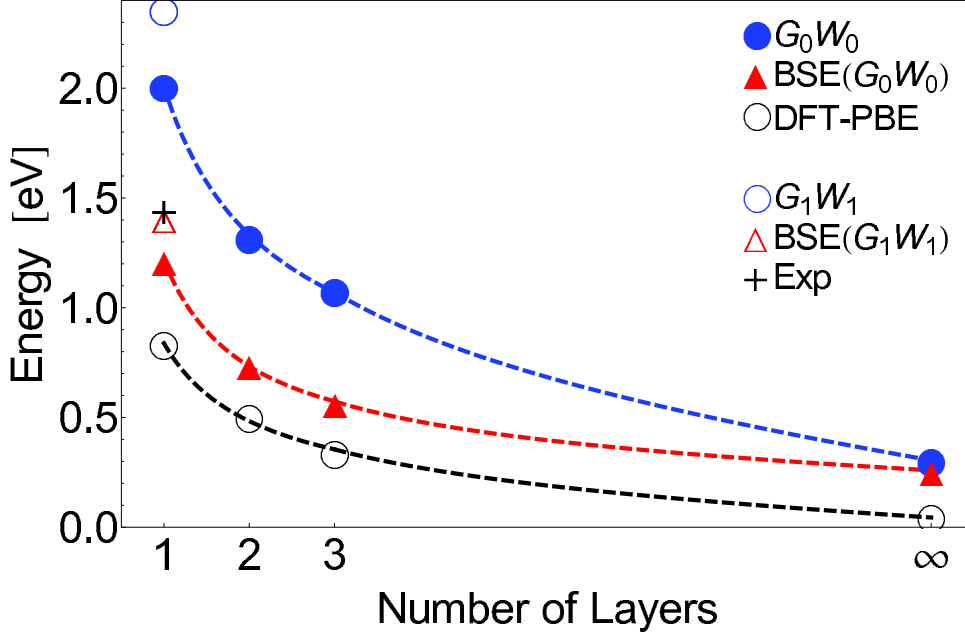


FIG. 2: (Color online) The evolution of band gap calculated by different methods and optical absorption peak according to the stacking layer number of few-layer phosphorene. The power-law fitting curves are presented by dashed lines. The experimental optical peak position is read from Ref. [5].

In all of the studied few-layer structures (Figs. 3 (a) to (c)), excitonic effects substantially reshape optical spectra; all of the main optical features are dominated by excitonic states. For example, in the monolayer structure, the first absorption peak is located at 1.2 eV, which is a strongly bound excitonic state with an 800-meV e - h binding energy. These exciton binding energies in phosphorene are comparable to those found in other monolayer semiconductors and 1D nanostructures [27, 30–32]. The reduced dimensionality and depressed screening are primary factors for fostering such enhanced excitonic effects.

Recently, a photoluminescence measurement of monolayer phosphorene was performed [5]. The measured spectral peak position (1.45 eV) is marked in Fig. 2; it resides slightly above our single-shot GW-BSE result. Self-consistently updating the Green’s function spectrum and dielectric function using the G_1W_1 methodology yields an exciton energy of 1.4 eV, as shown in Fig. 2. However, it should be noted that extrinsic factors may influence experimental data [5], which may account for some of the disagreement with our calculations. Therefore, additional experimental results must be assessed before further conclusions can be made.

TABLE I: Fitted parameters for band gaps, the first optical absorption peak (“optical gap”) and exciton binding energy of few-layer black phosphorus according to the formula $A/N^\alpha + B$.

	DFT/PBE	GW	Optical Gap	Binding Energy
α	0.85	0.73	0.96	0.53
A (eV)	0.79	1.70	0.87	0.83
B (eV)	0.04	0.30	0.28	0.03

In the bulk limit of black phosphorus, the optical absorption spectrum is nearly unchanged by the inclusion of e - h interactions (Fig. 3 (d)). Our simulation estimates the upper limit of the exciton binding energy as 30 meV, which is similar to those in other bulk semiconductors [17]. However, this is surprisingly different from similar layered materials. For example, bulk hexagonal BN possesses a significant exciton binding energy of 600 meV [24]. We attribute the small excitonic effects in bulk phosphorous to its stronger interlayer interactions, which is exhibited by its sizable interlayer band dispersion [13], making it a true three-dimensional material unlike other, more weakly coupled layer structures. We have also compared the electronic charge distributions of monolayer and bulk phosphorene. The interlayer interaction results in the reduction of interlayer distance and substantial out-plane features (see the details in the supplementary documents). This interlayer interaction and corresponding coupling reduce the perpendicular quantum confinement, resulting smaller band gaps and weaker excitonic effects.

The optical absorption spectra for light polarized along the zigzag direction of few-layer black phosphorous is presented in Fig. 4. These host profoundly-distinct absorption energy-ranges from the armchair spectra; the prominent absorption features begin at higher energies - near 2.8 eV. Thus monolayer phosphorene strongly absorbs armchair-polarized light with energies between 1.1 eV and 2.8 eV and is transparent to zigzag-polarized light in the same energy range; this phenomenon is the result of selection rules associated with the symmetries of this anisotropic material. Phosphorene is thus a natural optical linear polarizer, which can be used in liquid-crystal displays, three-dimensional visualization techniques, (bio)-dermatology, and in optical quantum computers [33, 34]. Furthermore, the polarization energy window is tunable through a wide range. Comparing Figs. 3 and 4, the high-end of

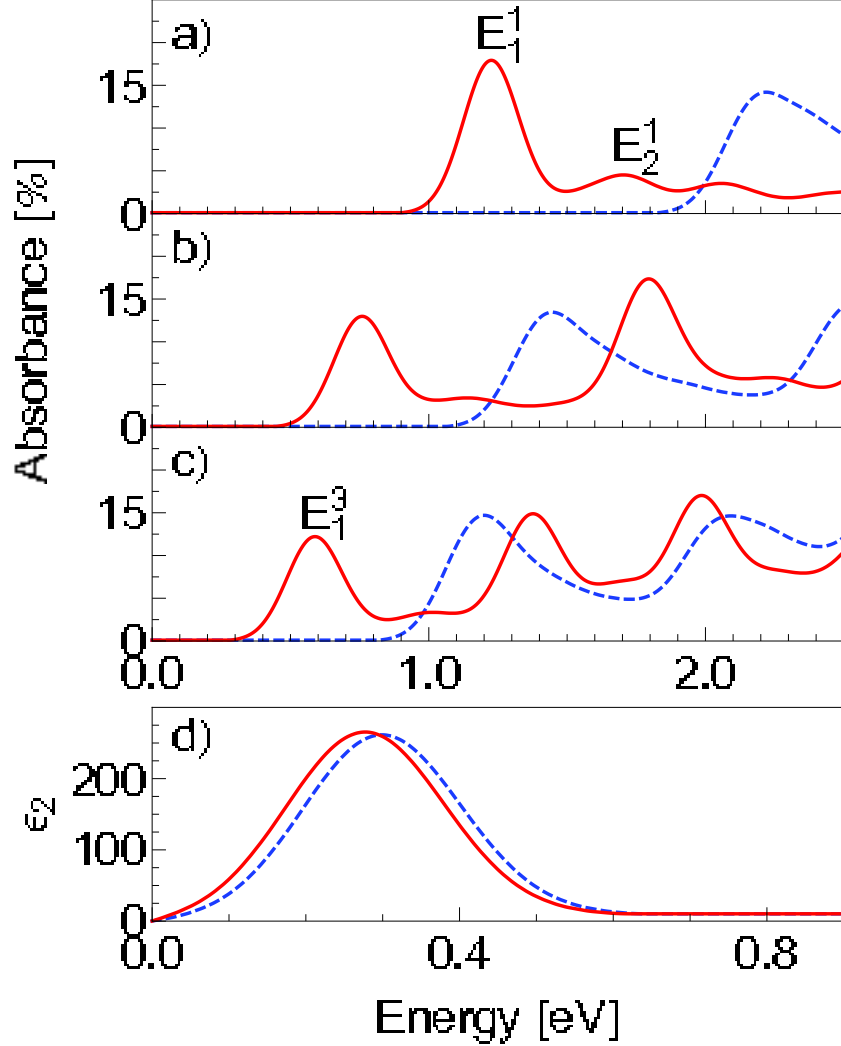


FIG. 3: (Color online) (a) to (d) Optical absorption spectra of monolayer, bilayer, trilayer, and bulk phosphorene for the incident light polarized along the x (armchair) direction. The single-particle optical absorption are presented by dashed lines while those spectra with e - h interaction included are presented by solid lines. We employ a 0.1 eV Gaussian smearing in these plots.

the polarization window is nearly fixed at 2.8 eV, while the low-end can be reduced from 1.1 eV down to 300 meV, by adjusting the layer stacking number. This frequency range is very exploitable for applications - it covers the infrared and near-infrared regimes. Finally, this anisotropic optical response can be used to identify the orientations of few-layer black phosphorous in experiments.

We have plotted wave functions of typical bright excitons in Fig. 5. An overall character of these excitons is that their spatial distribution of wave functions is anisotropic and, in

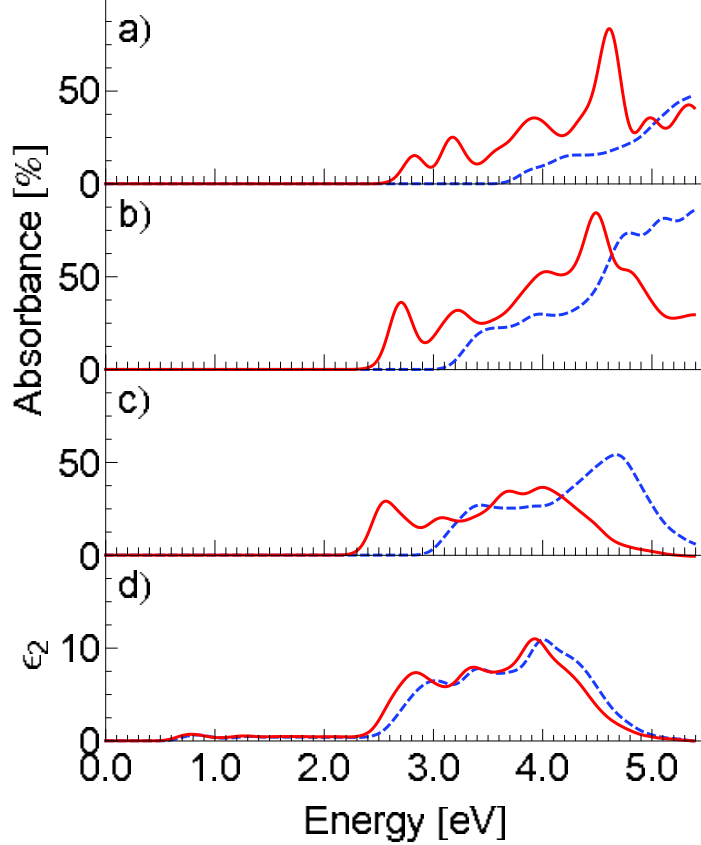


FIG. 4: (Color online) (a) to (d) Optical absorption spectra of monolayer, bilayer, trilayer, and bulk phosphorene for the incident light polarized along the y (zigzag) direction. The single-particle optical absorption are presented by dashed lines while those spectra with e - h interaction included are presented by solid lines.

particular, is extended along the armchair direction. This is consistent with the anisotropic band dispersion shown in Fig. 1 (b). These excitons form striped patterns, similar to those found in bundles of nanowires. This is due to the fact that the near-isotropic binding Coulomb interaction pulls on electrons that are mobile only along one direction. Interestingly, the optical activities of these plotted excitons are strongly correlated with their spacial anisotropy; they are optically bright only for the incident light polarized along the extended direction (armchair direction) of their wave function, if we compare Figs. 3, 4, and 5.

If we compare wavefunctions of the first two bright excitons (E_1^1 and E_2^1 marked in Fig. 3 (a)) from the same series in monolayer phosphorene (Figs. 5 (a) and (b)), we see that their respective distributions resemble one another both perpendicular to the structure and along the stripe direction (armchair axis). It should be noted that the second excitonic

state (E_2^1) has a clear nodal structure perpendicular to the stripe direction (along the zigzag axis), though one expects a 1D exciton to exhibit nodes along the stripe direction. The wave function of the first bright exciton (E_1^3) of trilayer phosphorene is plotted in Figs. 5 (c) and (e). Although the hole is fixed in one layer, electrons are distributed on both layers. Thus the spatial extent of, and the interactions between the excitons can also be controlled by the layer stacking number.

Finally, we assess the dependence of the many-electron effects on the interlayer distance and dimensionality. Our studies show that the interlayer distance slightly changes from bilayer to bulk black phosphorus (less than 0.8 %). Meanwhile, QP band gaps and intralayer excitons of suspended few-layer phosphorene (which is treated with a Coulomb truncation) are not very sensitive to the change of interlayer distances. For example, the band gap of bilayer phosphorene varies by less than 60 meV for the change of interlayer distance of $\pm 0.5\text{\AA}$. These many-electron effects are rooted in the vast vacuum that surrounds the isolated system, and are consequently not significantly affected by small changes of the interlayer distance. The layers of bulk black phosphorous, on the other hand, do not interface with a vacuum, and their excited state properties are sensitive to the interlayer distance. A small change of ($\pm 0.5\text{\AA}$) in the interlayer distance can shift the band gap and exciton energy by 150 meV, which is significant by comparison to the 300-meV band gap. (Additional details can be found in the supplementary document.) Obviously, if the thickness of few-layer black phosphorus is larger than the characteristic size of QPs or excitons, many-electron effects shall smoothly evolve to the bulk limit. Based on sizes of excitons plotted in Fig. 5, we estimate the critical thickness is around 10 nm, which is roughly around 20 layers.

In conclusion, first-principles simulations have been performed to determine the defining properties of few-layer black phosphorus and their exciting potential applications. Enhanced many-electron effects are essential in shaping their band gaps and optical responses because of anisotropic band dispersions and the effectively quasi-1D nature. In particular, our discovered uniquely anisotropic optical response with e - h interactions included makes phosphorene ideal for linear optical polarizers, covering the infrared and a part of visible light regime of broad interest. Finally, we show that all these properties can be efficiently tuned by the stacking layer number, which is potentially useful for device design.

We are supported by NSF Grant No. DMR-1207141. We acknowledge Erik Henriksen and Ruixiang Fei for fruitful discussions. The computational resources have been provided

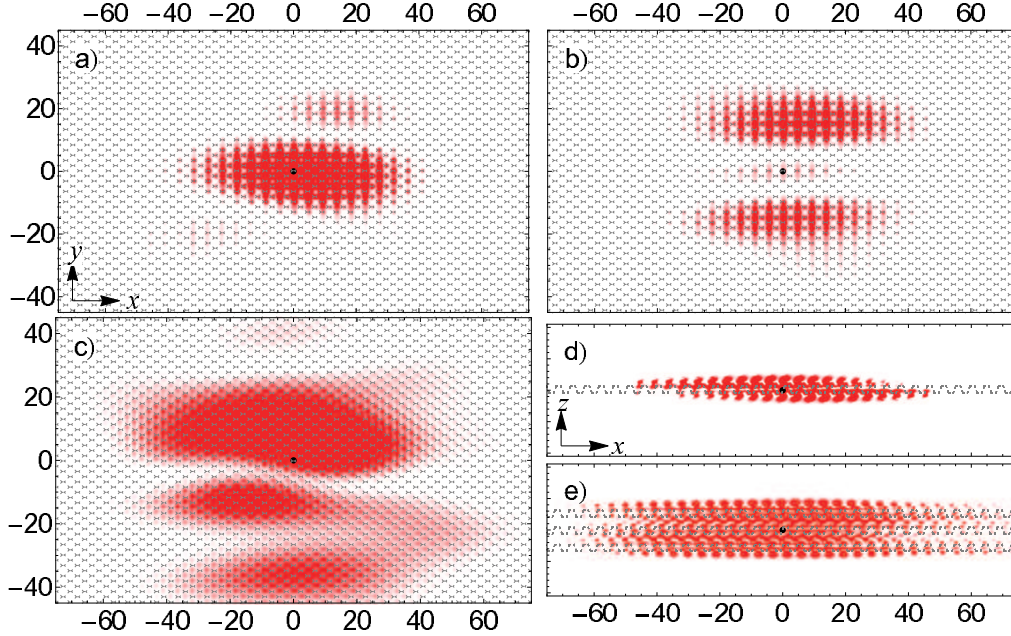


FIG. 5: (Color online) (a) and (b) Top views of the square of the electron wavefunctions of the first and second bound excitons in monolayer phosphorene (marked as E_1^1 and E_2^1 in Fig. 3 (a)). (c) Top view of the electron wavefunction of the first bound exciton in bilayer phosphorene (marked as E_1^3 in Fig. 3 (c)). (d) and (e) Side view of the wavefunctions in (a) and (c) respectively. The hole, represented by a black dot, is fixed at the origin. Lines representing the atomic bonds are superimposed. The scale is in angstroms.

by Lonestar of Teragrid at the Texas Advanced Computing Center. The ground state calculation is performed by the Quantum Espresso [35]. The GW-BSE calculation is done with the BerkeleyGW package [36].

-
- [1] K.S. Novoselov *et al.*, Science **306**, 666 (2004).
 - [2] A. K. Geim and K. S. Novoselov, Nature Materials **6**, 183-191 (2007).
 - [3] A. H. Castro Neto, *et al.*, Rev. Mod. Phys. **81**, 109 (2009).
 - [4] Likai Li, Yijun Yu, Guo Jun Ye, Qingqin Ge, Xuedong Ou, Hua Wu, Donglai Feng, Xian Hui Chen, and Yuanbo Zhang, Nature Nanotechnology (2014) doi:10.1038/nnano.2014.35.
 - [5] Han Liu, Adam T. Neal, Zhen Zhu, David Tomanek, and Peide D. Ye, ACS Nano, Article ASAP (2014), DOI: 10.1021/nn501226z.

- [6] Fengnian Xia, Han Wang, Yichen Jia, arXiv:1402.0270 (2014).
- [7] Eugenie Samuel Reich, Nature **506**, 19 (2014).
- [8] Jingsi Qiao, Xianghua Kong, Zhi-Xin Hu, Feng Yang, Wei Ji, arXiv:1401.5045 (2014).
- [9] A. Splendiani, L. Sun, Y. Zhang, T. Li, J. Kim, C.Y. Chim, G. Galli, and F. Wang, Nano letters **10**, 1271 (2010).
- [10] Sefaattin Tongay, Jian Zhou, Can Ataca, Kelvin Lo, Tyler S. Matthews, Jingbo Li, Jeffrey C. Grossman, and Junqiao Wu, Nano Lett., **12**, 5576 (2012).
- [11] C. Ataca, H. Sahin, and S. Ciraci, J. Phys. Chem. C **116**, 8983 (2012).
- [12] Allan Brown and Stig Rundqvist, Acta Cryst **19**, 684 (1965).
- [13] Y. Takao, H. Asahina, and A. Morita, Journal of Phys. Soc. of Jap. **50**, 3362 (1981).
- [14] John P. Perdew, Kieron Burke, and Matthias Ernzerhof, Phys. Rev. Lett. **77**, 3865 (1996).
- [15] N. Troullier and J. L. Martins, Phys. Rev. B **43**, 1993 (1991).
- [16] M.S. Hybertsen and S.G. Louie, Phys. Rev. B **34**, 5390 (1986).
- [17] M. Rohlfing, and S.G. Louie, Phys. Rev. B **62**, 4927 (2000).
- [18] S. Ismail-Beigi, Phys. Rev. B **73**, 233103 (2006).
- [19] C. A. Rozzi, D. Varsano, A. Marini, E. K. U. Gross, and A. Rubio, Phys. Rev. B **73**, 205119 (2006)
- [20] C. D. Spataru, S. Ismail-Beigi, L. X. Benedict, and S. G. Louie, Appl. Phys. A: Mater. Sci. Process. **78**, 1129 (2004).
- [21] Li Yang, C.D. Spataru, S.G. Louie, and M.Y. Chou, Phys. Rev. B **75**, 201304 (2007).
- [22] B. Radisavljevic, A. Radenovic, J. Brivio, V. Giacometti, A. Kis, Nature Nanotech **6**, 147 (2011).
- [23] Saptarshi Das, Hong-Yan Chen, Ashish Verma Penumatcha, and Joerg Appenzeller, Nano Lett. **13**, 100 (2013).
- [24] Ludger Wirtz, Andrea Marini, and Angel Rubio, Phys. Rev. Lett. **96**, 126104 (2006).
- [25] B. Arnaud, S. Lebe'gue, P. Rabiller, and M. Alouani, Phys. Rev. Lett. **96**, 026402 (2006).
- [26] A. Ramasubramaniam, Phys. Rev. B **86**, 115409 (2012).
- [27] Diana Y. Qiu, Felipe H. da Jornada, and Steven G. Louie, Phys. Rev. Lett. **111**, 216805 (2013).
- [28] Robert W. Keyes, Phys. Rev. **92**, 580 (1953).
- [29] Douglas Warschauer, Journal of Appl. Phys. **34**, 1853 (1963).

- [30] L. Yang, M. Cohen and S.G. Louie, *Nano Lett.* **7**, pp. 3312-3115, 2007.
- [31] C.D. Spataru, S. Ismail-Beigi, L. X. Benedict, and S.G. Louie, *Phys. Rev. Lett.* **92**, 077402 (2004).
- [32] F. Wang, G. Dukovic, L.E. Brus and T.F. Heinz, *Science* **308**, 838 (2005).
- [33] N. Zeng, X. Jiang, Q. Gao, Y. He, and H. Ma, *Appl Opt* **48**, 6734 (2009).
- [34] A. Knill, R. Laflamme, GJ Milburn, *Nature* **409**, 46 (2001).
- [35] P. Giannozzi *et al.*, *J. Phys.: Condens. Matter* **21**, 395502 (2009).
- [36] J. Deslippe *et al.*, *Comput. Phys. Commun.* **183**, 1269 (2012).